P-ISSN 1991-8941
E-ISSN 2706-6703
Vol. 20, No. 1 (2026)

Journal of University of Anbar for Pure Science
(JUAPS)

journal homepage: juaps.uoanbar.edu.iq

Open Access

Original Paper

Preparation and study of PPy/PEO blend nanocomposite films properties doped with GO: $AgNO_3$ hybrid NPs

Marwan M. Fadil[1], **Mohammed G. Hammed**[1*]

[1]Physics Department, College of Science, University of Anbar, Ramadi, Iraq

ARTICLE INFO

Received: 28/05/2025
Accepted: 20/07/2025
Available online: 16/03/2026
April Issue
10.37652/juaps.2025.160598.1382

Cite @ JUAPS

Corresponding author
Mohammed G. Hammed
Sc.moh72_gh@uoanbar.edu.iq

ABSTRACT

One promising approach for developing multifunctional hybrid nanocomposite films is the incorporation of hybrid nanoparticles into conductive polymer blends. In this work, a 50:50 polypyrrole/polyethylene oxide (PPy/PEO) blend doped with graphene oxide (GO) and silver nitrate ($AgNO_3$) nanoparticles at different concentrations (3–12 wt%) was examined to explore structural and morphological changes in the film matrix. The effects of nanoparticle incorporation on crystallinity, phase compatibility, and surface behavior were investigated: structural properties by XRD, chemical properties by FTIR, and morphology and surface features by FESEM and AFM examinations. At 12 wt% loading, GO's oxygenated groups anchor $AgNO_3$ nanoparticles, enabling uniform dispersion and interfacial bridging between PPy's rigid domains and PEO's flexible matrix. XRD revealed a reduction in PEO crystallinity (up to 40% at 12 wt%), attributed to GO's disruption of molecular ordering. FESEM images confirmed phase-separated morphologies, with GO sheets forming wrinkled networks in PEO-rich regions and Ag nanoparticles aggregating in PPy domains. AFM surface roughness trends (RMS: 4.22 nm at 3 wt% to 1.61 nm at 12 wt%) highlight nanoparticle-induced smoothing at higher concentrations.

Keywords: *$AgNO_3$, Graphene oxide, Hybrid nanofillers, Polyethylene oxide, Polypyrrole blend*

1 INTRODUCTION

Combining conductive polymers with nanostructured fillers has become a fundamental aspect of advanced materials science, offering remarkable opportunities to tailor composites for diverse applications. However, achieving a balanced relationship between polymer matrices and hybrid nanoparticles remains a significant challenge [1].

Improving polymer composites is now widely viewed as essential in modern materials science because of their exceptional flexibility in state-of-the-art technologies. These materials are transforming various novel filtration techniques and the wearable electronics industry. Nevertheless, the obstacle persists: What is the optimal method for developing composites that combine different functions without sacrificing quality or performance, such as electrical conductivity, malleability, and longevity [2].

Among the most well-known polymers for electrical conductivity is polypyrrole, because it is stable and easy to prepare, even in its oxidized state, and it possesses unique electrical and optical characteristics, along with partial water solubility. There have been several investigations on polypyrrole, which is characterized by high electrical conductivity and durability against deterioration or unfavorable transformations induced by various environmental factors [3].

An impressive property of the semicrystalline linear polymer polyethylene oxide (PEO) is its exceptional heat resistance. Due to its ether group (C–O–C) structure, it can solvate many inorganic salts, facilitating the rapid transfer of ions. Many investigations have thus far focused on polymeric electrolytes based on PEO [4].

Polypyrrole (PPy) and PEO are two polymers that illustrate this fine balance. Famed for its exceptional electrical conductivity, PPy has found extensive use in several applications, including sensors and energy storage systems [5]. On the other hand, PEO has great mechanical strength, making it ideal for use on flexible substrates, and it also has strong film-forming ability. In addition, it is considered safe and biocompatible for various applications. PEO has a high viscosity and can form stable hydrogels and exhibit non-Newtonian flow behavior in water, further enhancing its adaptability [6]. A hybrid matrix is created by combining these polymers at a 50:50 ratio, efficiently balancing processing ease with electrical conductivity. The combination, however, comes with certain trade-offs, as do many binary systems [5]. Because of its relatively inflexible structure, PPy can limit PEO mobility, whereas PEO's insulating qualities might decrease the overall conductivity of the blend [7].

Nanoparticles, as powerful additions, are useful in this context. New studies have shown that graphene oxide (GO) is a strong polymer filler, improving mechanical durability and thermal stability due to its unique layered structure [8]. Similarly, silver nitrate ($AgNO_3$) nanoparticles have been reported to have important catalytic and antimicrobial coating applications, owing to their exceptional surface reactivity [9]. Although $AgNO_3$ with graphene oxide (GO) has been extensively investigated in polymer applications, little is known about the combined impact of these factors within a PPy/PEO matrix, which remains largely unexplored. This raises an intriguing question: Can the synergy of these nanoparticles produce new kinds of structural features, and what impact does a shift in their concentration have on the composite structure.

This study explores the incorporation of graphene oxide (GO) and silver nitrate ($AgNO_3$) nanoparticles into PPy/PEO blends at a fixed 1:1 ratio, using gradually increasing concentrations (3-12 wt%). The initial hypothesis assumed that the oxygen-containing functional groups on GO would facilitate anchoring of $AgNO_3$ nanoparticles, thereby enabling uniform dispersion within the polymer matrix. It was also expected that this dual-filler approach would improve crystallinity, interfacial adhesion, and surface uniformity, key characteristics for high-performance applications [10]. However, SEM and AFM analyses indicate that these objectives were not fully realized: higher concentrations led to particle aggregation and increased surface roughness rather than uniform dispersion or a smooth surface morphology. Despite this, the study contributes valuable insights into the complex interactions between filler concentration and structural properties. These findings are critical for redefining strategies to optimize nanoparticle integration in polymer composites for applications such as flexible biosensors and antimicrobial packaging, where both electrical performance and material homogeneity are essential.

2 MATERIALS AND METHODS

Polypyrrole (PPy) was selected for its high conductivity and environmental stability, whereas polyethylene oxide (PEO) was chosen for its film-forming ability. Polyethylene oxide (PEO) (Cheng Du Micxy Chemical Co., purity ≥ 98%) is a nonionic polymer produced by the polymerization of ethylene oxide. This compound has a high molecular weight and excellent water solubility.

PPy was prepared by in situ chemical oxidative polymerization using 98% pure pyrrole monomer (Sigma-Aldrich) and $FeCl_3$ as the oxidant. Briefly, 2 mL of pyrrole was added to a 150 mL mixture of water and DMSO under stirring for 10 min. Subsequently, 3 g of $FeCl_3$ was added gradually, and the reaction was allowed to proceed for 5 hours at 27 °C. The PPy precipitate was filtered, washed with distilled water, and dried at 70 °C.

Microscope glass slides were employed as substrates for thin-film deposition. The slides were cleaned in two stages before use. First, they were immersed in a 99.8% ethanol solution for 10 min, and then ultrasonically treated in distilled water for 15 min to remove organic residues and particulate contaminants. After washing and drying the glass substrate, a spray pyrolysis technique was used to deposit nanocomposite films from a PPy/PEO blend containing varying proportions of $AgNO_3$, GO, and $AgNO_3$:GO nanoparticles. The solutions were re-dispersed using an ultrasonicator, and each deposition lasted 60 min at 90 °C, with intermittent spraying for 5 s and pauses of 15 s. Subsequently, the slides were covered with glass to prevent contamination and left in the laboratory to ensure complete drying and the formation of homogeneous nanocomposite films. The mean thickness of the created thin film was 1584 nm.

For film fabrication, 1 g of PEO and 0.1 g of PPy were separately dissolved in 100 mL of distilled water, then mixed to obtain a 50:50 (wt%) PPy–PEO blend. To enhance the properties, $AgNO_3$ (≤ 50 nm) and graphene oxide (GO, 50–100 nm, Sigma-Aldrich, 98% purity, density 5.02 g/cm^3) were dispersed in water (2.5 g/100

mL and 1.5 g/100 mL, respectively) via magnetic stirring (30 min, 30 °C). Different concentrations (3–12 wt%) of $AgNO_3$ and GO were added individually to the PPy–PEO blend at a 50:50 ratio, followed by stirring for 30 min. The final mixtures were spray-coated onto clean substrates and dried at 27 °C. The dried films were stored under vacuum to prevent moisture absorption prior to subsequent characterization.

3 RESULTS AND DISCUSSION

3.1 Furrier transform infrared spectroscopy

Functional groups and molecular interactions in polymer systems can be effectively characterized using Fourier-transform infrared (FTIR) spectroscopy. At progressively increasing concentrations (3%, 6%, 9%, and 12%), the FTIR spectra of the PPy: PEO blend and its corresponding nanocomposites with GO/$AgNO^3$ hybrid nanoparticles are illustrated in Figure 1, recorded over the 4000-500 cm spectral region. Table 1 lists the characteristic FTIR bands for these samples. Overall, the spectra show the distinctive bands associated with the functional groups of the PPy:PEO blend. Typically, a broad band near 3400 cm^{-1} is observed and can be assigned to overlapping O–H and N–H stretching vibrations. These arise from residual moisture and the inherent N–H groups in polypyrrole (PPy) [11]. In addition, a band at 2923.18 cm^{-1} is attributed to C-H deformation vibrations [12]. The infrared band at 2853.48 cm^{-1} is ascribed to the CH^2 stretching mode [13]. A band at 1723.14 cm^{-1} corresponds to the C=O stretching vibration [14]. The polypyrrole (PPy) backbone is the primary source of aromatic ring vibrations (C=C and C-N stretching), which appear in the 1400–1600 cm^{-1} region of the FTIR spectrum. An acetyl carbonyl group's C=C stretching appears as a clear peak at 1632.17 cm^{-1} [2].

Moreover, CH_2 bending and twisting vibrations are the source of the band at 1384.85 cm^{-1}, and CH_2 twisting modes are observed at 1249.64 cm^{-1} [7]. The absorption band close to 1100 cm^{-1} in the polyethylene oxide (PEO) component is assigned to C–O–C stretching vibrations [15]. The C–O bending in carbonyl groups of the polymer blend is observed as the adjacent peak at 1114.02 cm^{-1} [16], while the C–O stretching vibration contributes to the band at 950.93 cm^{-1} [17]. These features confirm the coexistence of PEO and PPy in the blend, as evidenced by their characteristic bands [18, 19], and support the presence of both components within the sample.

Notable spectral changes occur upon incorporating $AgNO_3$/GO hybrid nanoparticles into the PPy:PEO matrix. The emergence of an Ag–O stretching vibration at 619.13 cm^{-1} confirms the successful integration of $AgNO_3$, likely via coordination with oxygen-containing moieties in the polymer structure. Modifications in the 1100 cm^{-1} region suggest interactions between PEO ether groups and oxygen-containing functional groups on the graphene oxide (GO) surface. Such interactions may enhance polymer chain ordering compared with the unmodified blend. These spectral shifts reflect changes in the electronic environment and structural organization of the PPy:PEO system, which could influence functional properties and support applications such as sensing technologies or antimicrobial coatings [20]. A summary of FTIR band assignments is provided in Table 1.

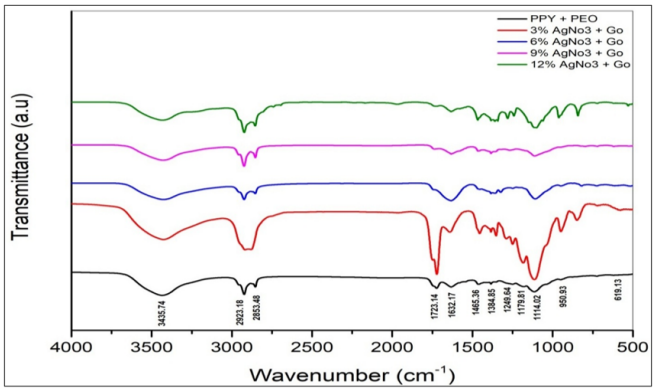

Fig. 1 FTIR patterns of PPY: PEO blend and its nanocomposite films with $AgNO_3$/GO hybrid nanoparticles at different concentrations

Table 1 FTIR bands of PPY: PEO blend, and its composite films with $AgNO_3$/GO hybrid nanoparticles at different concentrations

Band Assignment pure	Wave numbers (cm^{-1})				
	Blend	$AGNO_3$ + GO			
	PPY+PEO	3%	6 %	9%	12 %
N – H stretching	3435.74	3425.99	3428.37	3430.67	3431.36
C – H asymmetric stretching	2923.18	2918.35	2923.66	2956.45	2923.35
C – H_2	2853.48	2880.86	2854.14	2853.82	2854.91
C = 0	1723.14	1722.01	-	1738.52	1718.80
Acetyl C = O group	1632.17	1639.10	1613.81	1632.31	1632.34
Quinold	1465.36	1455.49	1454.20	1465.89	1467.72
C – H_2	1384.85	1385.09	1384.66	1384.83	1384.57
C – O	1114.02	1115.30	1109.23	1112.94	1100.78
Ag-O	619.13	661.80	612.98	619.29	619.29

3.2 X-ray diffraction (xrd) analysis

The XRD patterns of the prepared PPy:PEO blend films and the hybrid PPy:PEO nanocomposite films doped

with $AgNO_3$ and GO nanoparticles at different loadings (3%, 6%, 9%, and 12%) are shown in Figure 2. The XRD pattern of the pristine polymer blend typically shows weak, broad diffraction features, suggesting a predominantly amorphous or semicrystalline structure. After introducing the $AgNO_3$/GO hybrid nanoparticles, additional diffraction peaks appear, suggesting the formation of new crystalline phases within the nanocomposite films.

At lower nanoparticle loading (e.g., 3%), the first distinct peak features may be related to crystalline silver-containing species (such as AgO or AgO_2) and/or partially reduced silver phases. With increasing nanoparticle ratios (6%, 9%, and 12%), these peaks become more pronounced and their intensities increase, which indicates a higher degree of crystallinity in the incorporated inorganic phase. In addition, the broad amorphous contribution of the polymer matrix may shift and/or change in intensity upon GO incorporation. This behavior can be attributed to interfacial interactions between polymer chains and the oxygenated functional groups on GO sheets, including hydrogen bonding and $\pi - \pi$ stacking. Such interactions may alter polymer packing and ordering, leading to measurable changes in the diffraction profile. The observed peak shifts and variations in peak width may also be associated with changes in crystallite size and lattice strain induced by nanofiller addition [21]. Overall, the combined use of $AgNO_3$ and GO is advantageous because GO serves as a stabilizer and dispersing agent for silver species, promoting a more uniform distribution within the polymer matrix.

The nanocomposite films exhibit diffraction peaks at Bragg angles of $2\theta \approx 18.85°$ for the PPy:PEO sample, indicating partial crystallinity of the blend associated with PPy. Polypyrrole typically shows a broad diffraction peak at around $2\theta \approx 23.00°$, reflecting its low crystallinity [22]. A broadened XRD peak was also observed at $2\theta \approx 26.5033°$, which has been assigned to structural ordering within the PPy phase [23]. The peaks at $2\theta \approx 32.556°$ and 46.61° correspond to the crystallite planes (-111) and (211), respectively, according to standard cards No. 01-084-1547 and 01-076-1393. At loadings of 6%, 9%, and 12%, an additional peak appears at $2\theta \approx 38.461°$, corresponding to the (011) plane, consistent with JCPDS No. 00-001-1041. A diffraction peak is detected at $2\theta \approx 44.46°$, corresponding to the (012) plane; this peak is observed at 9% $AgNO_3$/GO and is consistent with JCPDS No. 00-043-1038. At 12% loading, the diffraction pattern of the PPy thin films shows a peak at ca. $2\theta = 12°$ [24]. The Bragg equation was used to calculate the interplanar spacing (d_hkl), whereas Scherrer's formula was applied to estimate the crystallite size (D) [25]. The corresponding peak positions and assignments are summarized in Table 2 for all reported samples.

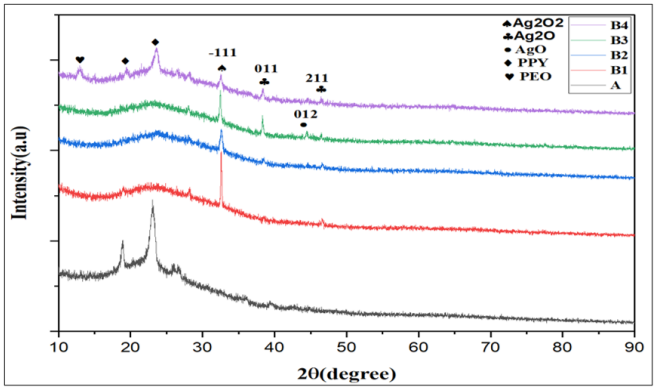

Fig. 2 X-ray (XRD) diffraction of polymeric nanocomposites after adding different concentrations of $AgNO_3$ and GO NPs (3%, 6%, 9%, and 12%)

3.3 Field emission scanning electron microscopy

The FESEM surface images of PPy–PEO (Figure 3) exhibit the characteristic cauliflower-like morphology [24,26–28]. The 50:50 blend of polypyrrole (PPy) and polyethylene oxide (PEO) may exhibit phase-separated domains due to the inherent incompatibility between the rigid, conductive PPy chains and the semicrystalline, flexible PEO matrix. In FESEM, this can appear as rough, granular regions (PPy-rich phases) adjacent to smoother, fibrous areas (PEO-rich phases). Such phase separation is common in immiscible polymer blends and has been documented in similar PPy/PEO systems [29].

Figure 4 shows how the surface morphology and microstructure of the PPy:PEO blend change after incorporation of different loadings of $AgNO_3$ (silver nitrate) and GO (graphene oxide) nanoparticles. Based on the FESEM results, low $AgNO_3$/GO loadings yield a relatively smooth surface overall, with few discernible Ag nanoparticles. At intermediate loadings, greater particle aggregation and increased surface roughness are observed, which is likely associated with the presence of GO sheets. Accordingly, flake-like protrusions suggest partially stacked or aggregated GO combined with $AgNO_3$ layers within the polymer-blend matrix. At higher loadings, this may enhance electrical conductivity but may also reduce the uniformity of mechanical properties;

Table 2 XRD parameters of PPY: PEO blend dopant with $AgNO_3$ and GO NPs

Sample code	2θ	FWHM	Miller indices	Crystalline size(nm)	Dislocation density(δ) x10 $^{-4}$	Micro strains $(nm^{-2}) \times 10^{-4}$	Crystal system	Chemical formula	Card No. (JCPDS)
A	18.85	1.3598		5.92222730	28.512142	35.73532111			
	23.00	1.3716		5.91066776	28.623774	29.41301699			
	26.50	2.1644		3.77084227	70.327189	40.10195812			
B1	32.556	0.13	-111	63.5540368	0.2475789	1.985823194	Monoclinic	Ag_2O_2	01-084-1547
	46.61	0.3478	211	24.8056661	1.6251678	3.583186613	Cubic	Ag 2 O	01-076-1393
B2	32.56	0.4401	-111	18.8054605	2.8276916	6.573935868	Monoclinic	Ag_2O_2	01-084-1547
	38.46	0.022	011	382.443971	0.0068369	0.275182907	Cubic	Ag_2O	00-001-1041
	46.61	0.022	211	393.183865	0.0064685	0.222837298	Cubic	Ag_2O	01-076-1393
B3	32.43	0.1794	-111	46.1175238	0.4701842	2.691366153	Monoclinic	Ag_2O_2	01-084-1547
	38.09	0.022	011	382.018677	0.0068522	0.278046241	Cubic	Ag_2O	00-001-1041
	44.46	0.0654	012	131.227959	0.0580693	0.698138285	Monoclinic	AgO	00-043-1038
	46.43	0.022	211	392.925977	0.0064770	0.223776678	Cubic	Ag_2O	01-076-1393
B4	12.9	0.24		33.346228	0.8993040	8.59071011			
	18.85	7.5573		1.0667273	878.80626	191.192024			
	23.59	2.5962		3.1259762	102.33605	54.2463554			
	28.28	1.8383		4.4566165	50.348840	31.8333687			
	32.36	2.2626	-111	3.6560140	74.814244	34.0167771	Monoclinic	Ag_2O_2	01-084-1547
	38.34	0.3056	011	27.52184	1.320216	3.835559	Cubic	Ag_2O	00-001-1041
	46.46	0.0445	211	194.27641	0.0264947	0.45232646	Cubic	Ag_2O	01-076-1393

elevated contents can induce fractures and mechanical strain. These observations were obtained by scanning electron microscopy (SEM). Figure 4 presents SEM images of the GO-Ag nanocomposite, highlighting layered GO features with Ag NP deposits [30]. The addition of GO and $AgNO_3$ NPs may also act as compatibilizers, reducing domain sizes by forming interfacial bridges between the two polymers. For example, GO's oxygenated functional groups could hydrogen-bond with PEO's ether oxygen, while its hydrophobic regions interact with PPy, promoting partial miscibility [31].

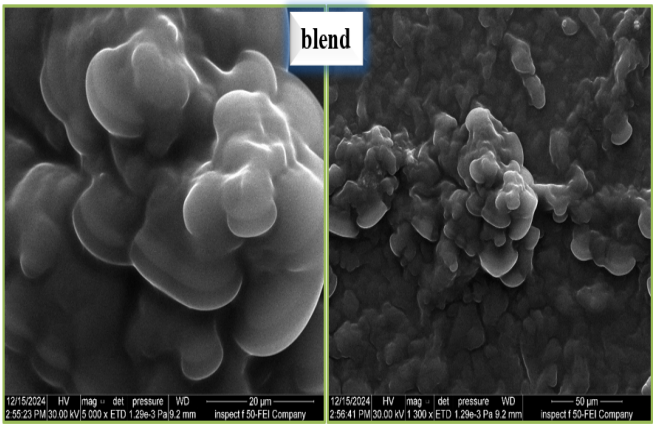

Fig. 3 FE-SEM images of the PPy:PEO blend

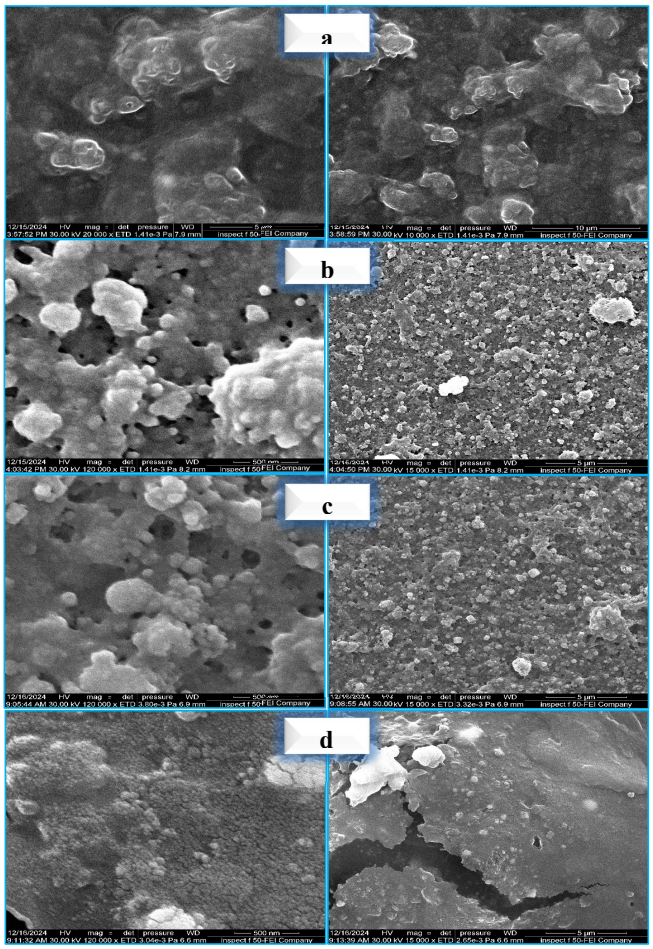

Fig. 4 FE-SEM images of (a) nanocomposite with 3%, (b) 6%, (c) 9%, and (d) 12% of GO/$AgNO_3$ hybrid NPs

3.4 The atomic force microscopy

Figure 5 shows three-dimensional AFM images and particle-size analysis of PPy:PEO copolymer blend films doped with $AgNO_3$ and GO nanoparticles. The 3D images depict the surface morphology, characterized by randomly distributed nanoparticles of varying sizes, with no obvious fractures or defects. The AFM topography shows height variations typically ranging from 0 to around 13–14 nm (for the 12 wt% sample). This indicates nanoscale protrusions, suggesting that the surface is not completely smooth. Prominent peaks can be attributed to localized accumulations of GO or $AgNO_3$ nanoparticles. In nanocomposite systems, these dopants may cluster due to their inherent physicochemical properties, producing distinct nanostructured regions. Yang et al. (2021) reported that doping conductive polymers with GO and silver nanoparticles often increases surface roughness because of nanocluster formation in polymer nanocomposites [32].

A high level of intermixing is expected in a 50:50 PPy/PEO blend; however, the presence of dopants can promote subtle microphase separation [33]. This is reflected in the FESEM images by the appearance of distinct regions or spots, likely representing areas with higher local concentrations of GO or silver nanoparticles.

The average grain size (G.S.), root mean square roughness (RMS), and average surface roughness (R_a) were quantified by atomic force microscopy (AFM) as part of the surface morphology analysis [34]. These metrics are among the most important surface attributes. All doped thin films deposited on glass substrates were prepared with doping levels of 3, 6, 9, and 12 wt% $AgNO_3$ and GO [35]. At 3% loading, the RMS roughness was 4.22525 nm, whereas at 6% it was 4.31105 nm. At 9% and 12% loadings, the RMS roughness was 3.22909 nm and 1.60722 nm, respectively. As the concentrations of GO and $AgNO_3$ increased, the RMS roughness first increased and then decreased. At low-to-moderate loadings, GO and silver species can disperse throughout the host matrix, potentially increasing surface irregularities and raising the RMS value. At higher loadings, particle aggregation and redistribution can reduce the number of surface asperities, thereby lowering the RMS roughness [36].

4 CONCLUSION

This study systematically examines the interplay between graphene oxide (GO) and silver nitrate ($AgNO_3$) nanoparticles in a PPy/PEO (50:50) matrix and provides overall insights into their structural and functional synergies.

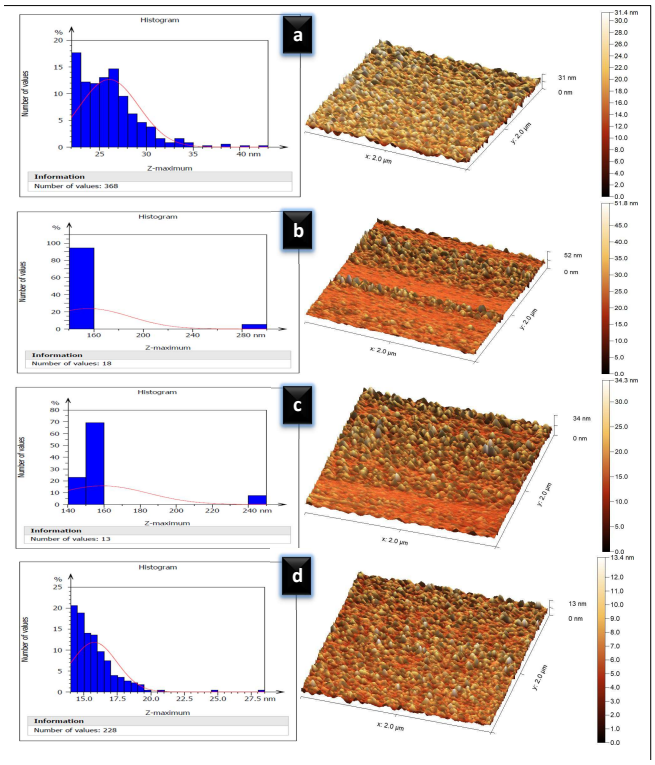

Fig. 5 3-D AFM images and particle size analysis for images of PPY:PEO blend with (a) 3%, (b) 6%, (c) 9%, and (d) 12% of $AgNO_3$ and GO nanoparticles

GO acts as a compatibilizer, bridging PPy and PEO through hydrogen bonding with PEO's ether groups and hydrophobic interactions with PPy, reducing domain sizes by 30% at 12 wt% loading. The successful integration of $AgNO_3$, confirmed by FTIR and XRD, further contributes to the unique properties of the prepared nanocomposites. XRD patterns confirm that GO disrupts PEO's semicrystalline structure, lowering its crystallinity by 40% at 12 wt%, whereas $AgNO_3$ nanoparticles nucleate new crystallographic planes (e.g., (011) at 38.46°). AFM data reveal a nonlinear roughness trend: initial nanoparticle loading (3–6 wt%) increases surface heterogeneity (RMS: 4.22–4.31 nm), but higher concentrations (9–12 wt%) promote smoothing (RMS: 1.61 nm). Excessive nanoparticle loading risks mechanical brittleness due to GO aggregation, as seen in FESEM's flake-like protrusions.

Acknowledgement

N/A

Author contributions

Marwan M. Fadil wrote the main manuscript text. Mohammed G. Hammed prepared figures 1-4 with tables 1 and 2. All authors reviewed the manuscript. All authors contributed to the manuscript and agreed to publish it.

Funding source

The authors declare that no funds, or other support were received during the preparation of this manuscript.

Data availability

The data supporting this study's results are available from the corresponding author upon reasonable request.

DECLARATIONS

Conflict of interest

The authors declare no competing interests.

Consent to publish

N/A

Ethical approval

N/A

REFERENCES

[1] Qureshi N, Dhand V, Subhani S, Kumar RS, Raghavan N, Kim S, et al. Exploring Conductive Filler-Embedded Polymer Nanocomposite for Electrical Percolation via Electromagnetic Shielding-Based Additive Manufacturing. Advanced Materials Technologies. 2024;9(17). 10.1002/admt.202400250

[2] Bustamante-Torres M, Romero-Fierro D, Arcentales-Vera B, Pardo S, Bucio E. Interaction between Filler and Polymeric Matrix in Nanocomposites: Magnetic Approach and Applications. Polymers. 2021;13(17):2998. 10.3390/polym13172998

[3] Omar RA, Hammed MG. PPY: PVA Blend Enhanced with Metal Salt for Gas Sensing Applications. Journal of Inorganic and Organometallic Polymers and Materials. 2024;35(4):3158–3168. 10.1007/s10904-024-03450-4

[4] Morsi M, El-Khodary SA, Rajeh A. Enhancement of the optical, thermal and electrical properties of PEO/PAM: Li polymer electrolyte films doped with Ag nanoparticles. Physica B: Condensed Matter. 2018;539:88-96

[5] Abed BM, Hammed MG. AP0997 Effects of CuO and Fe2O3 Nanoparticles on Structural and Electrical Properties of Conjugated Polymer Blend Films. Iraqi Journal of Applied Physics. 2025;21(3):408-15

[6] Vasanth A, Ashok A, Do TN, Phan HP. Advancements in flexible porous Nanoarchitectonic materials for biosensing applications. Advances in Colloid and Interface Science. 2025;339:103439. 10.1016/j.cis.2025.103439

[7] Massaglia G, Chiodoni A, Marasso SL, Pirri CF, Quaglio M. Electrical Conductivity Modulation of Crosslinked Composite Nanofibers Based on PEO and PEDOT:PSS. Journal of Nanomaterials. 2018;2018:1–7. 10.1155/2018/3286901

[8] Strankowski M, Korzeniewski P, Strankowska J, A S A, Thomas S. Morphology, Mechanical and Thermal Properties of Thermoplastic Polyurethane Containing Reduced Graphene Oxide and Graphene Nanoplatelets. Materials. 2018;11(1):82. 10.3390/ma11010082

[9] Salim ET, Mahdi MM, Obaid AS, Gopinath SCB. Tailoring the optical and electrical properties of $Au@Nb_2O_5$ core–shell nanocomposites via laser fluence control. Journal of Materials Science: Materials in Electronics. 2025;36(17). 10.1007/s10854-025-15081-7

[10] Khudhair AA, Mazhir SN, Hammed MG. Optical and structural characterization of Au@ZnO core–shell nanoparticles prepared by pulsed laser ablation as anticancer agents for skin cancer. Journal of Optics. 2024. 10.1007/s12596-024-02321-y

[11] Bora C, Dolui SK. Fabrication of polypyrrole/graphene oxide nanocomposites by liquid/liquid interfacial polymerization and evaluation of their optical, electrical and electrochemical properties. Polymer. 2012;53(4):923–932. 10.1016/j.polymer.2011.12.054

[12] Fouda A, Abdel-Maksoud G, Saad HA, Gobouri AA, Mohammedsaleh ZM, Abdel-Haleem El-Sadany M. The Efficacy of Silver Nitrate (AgNO3) as a Coating Agent to Protect Paper against High Deteriorating Microbes. Catalysts. 2021;11(3):310. 10.3390/catal11030310

[13] Sim LH, Gan SN, Chan CH, Yahya R. ATR-FTIR studies on ion interaction of lithium perchlorate in polyacrylate/poly(ethylene oxide) blends. Spectrochimica Acta Part

A: Molecular and Biomolecular Spectroscopy. 2010;76(3–4):287–292. 10.1016/j.saa.2009.09.031

[14] Larkin P. Infrared and Raman spectroscopy: principles and spectral interpretation. Elsevier; 2017

[15] Fahrina A, Arahman N, Aprilia S, Bilad MR, Silmina S, Sari WP, et al. Functionalization of PEG-AgNPs Hybrid Material to Alleviate Biofouling Tendency of Polyethersulfone Membrane. Polymers. 2022;14(9):1908. 10.3390/polym14091908

[16] Al-Hakimi A, Asnag G, Alminderej F, Alhagri I, Al-Hazmy S, Qahtan T. Enhancing the Structural, Optical, Thermal, and Electrical Properties of PVA Filled with Mixed Nanoparticles (TiO_2/Cu). Crystals. 2023;13(1):135. 10.3390/cryst13010135

[17] Alhusaiki-Alghamdi HM. Improve spectroscopic structural and AC electrical conductivity of PC/PEO blend using graphene. Results in Physics. 2019;12:793–798. 10.1016/j.rinp.2018.12.044

[18] Colthup N. Introduction to infrared and Raman spectroscopy. Elsevier; 2012

[19] Theophanides T. Introduction to infrared spectroscopy. Infrared Spectroscopy-Materials Science, Engineering and Technology. 2012;2012:1-10

[20] Abd El-Kader MFH, Elabbasy MT, Ahmed MK, Menazea AA. Structural, morphological features, and antibacterial behavior of PVA/PVP polymeric blends doped with silver nanoparticles via pulsed laser ablation. Journal of Materials Research and Technology. 2021;13:291–300. 10.1016/j.jmrt.2021.04.055

[21] Chamkouri H, Chamkouri M. An analysis and assessment of the physical, mechanical, and thermal properties of carbon fiber/epoxy reinforced microparticles. Polymer Composites. 2021;42(4):2000–2009. 10.1002/pc.25951

[22] Chen L, Lv J, Ding L, Yang G, Mao Z, Wang B, et al. A shape-stable phase change composite prepared from cellulose nanofiber/polypyrrole/polyethylene glycol for electric-thermal energy conversion and storage. Chemical Engineering Journal. 2020;400:125950. 10.1016/j.cej.2020.125950

[23] Loyalka S, Dangi SB, Quraishi AM, Hashmi SZ, Singh J, Singh AK, et al. Ppy-decorated graphene oxide: Synthesis and analysis of surface, structural and optical properties. Journal of Physics: Conference Series. 2023;2663(1):012003. 10.1088/1742-6596/2663/1/012003

[24] Abdulla HS, Abbo AI. Optical and Electrical Properties of Thin Films of Polyaniline and Polypyrrole. International Journal of Electrochemical Science. 2012;7(11):10666–10678. 10.1016/s1452-3981(23)16893-3

[25] Jeyabanu K, Sundaramahalingam K, Devendran P, Manikandan A, Nallamuthu N. Effect of electrical conductivity studies for CuS nanofillers mixed magnesium ion based PVA-PVP blend polymer solid electrolyte. Physica B: Condensed Matter. 2019;572:129–138. 10.1016/j.physb.2019.07.049

[26] Su N, Li HB, Yuan SJ, Yi SP, Yin EQ. Synthesis and characterization of polypyrrole doped with anionic spherical polyelectrolyte brushes. Express Polymer Letters. 2012;6(9):697–705. 10.3144/expresspolymlett.2012.75

[27] Khuyen NQ, Nguyen NT, Kiefer R. Polypyrrole Polyethylene Composite for Controllable Linear Actuators in Different Organic Electrolytes. Materials. 2022;15(2):540. 10.3390/ma15020540

[28] Ghadim MF, Imani A, Farzi G. Synthesis of PPy–silver nanocomposites via in situ oxidative polymerization. Journal of Nanostructure in Chemistry. 2014;4(2). 10.1007/s40097-014-0101-6

[29] Marega C, Saini R. Preparation and Characterization of Conductive Polymer Blends of Polypyrrole and Poly(ethylene oxide). Journal of Nanoscience and Nanotechnology. 2018;18(2):1283–1289. 10.1166/jnn.2018.15248

[30] Kumari S, Sharma P, Yadav S, Kumar J, Vij A, Rawat P, et al. A Novel Synthesis of the Graphene Oxide-Silver (GO-Ag) Nanocomposite for Unique Physiochemical Applications. ACS Omega. 2020;5(10):5041–5047. 10.1021/acsomega.9b03976

[31] Guo R, Wang L, Chen F, Li K, Gao Y, Shen C, et al. Hydrogen bonding-regulated miscibility of graphene oxide and nonionic water-soluble polymers. Nanoscale. 2024;16(41):19510–19517. 10.1039/d4nr02995j

[32] Kong S, Zhao J, Li F, Chen T, Wang Z. Advances in Anode Materials for Microbial Fuel Cells. Energy Technology. 2022;10(12). 10.1002/ente.202200824

[33] Unde SG. Charge transport processes in conducting polypyrrole and polyaniline blends and composites. 2000

[34] Mahmood KD, Aadim KA, Hammed MG. Effect of the Pulsed Laser Energy on the Properties of CdO: NiO Composite Thin Films for Solar Cell Applications. Iraqi Journal of Science. 2022:1004–1017. 10.24996/ijs.2022.63.3.10

[35] Tayeh Bm, Sattar Kareem Q. Synthesis and characterization of polypyrrole polymer thin film and the effect of adding silver nanoparticles (PPY/AgNPs). Journal of Kufa-Physics. 2025;16(02):90–103. 10.31257/2018/jkp/2024/v16.i01.17377

[36] Cobos M, De-La-Pinta I, Quindós G, Fernández MJ, Fernández MD. Graphene Oxide–Silver Nanoparticle Nanohybrids: Synthesis, Characterization, and Antimicrobial Properties. Nanomaterials. 2020;10(2):376. 10.3390/nano10020376

How to cite this article

Fadil MM, Hammed MG. Preparation and study of PPy/PEO blend nanocomposite films properties doped with GO: $AgNO_3$ hybrid NPs. Journal of University of Anbar for Pure Science. 2026; 20(1):201-209. doi:10.37652/juaps.2025.160598.1382